DMD Fast Forward. Published on August 18, 2017 as DOI: 10.1124/dmd.117.076349
This article has not been copyedited and formatted. The final version may differ from this version.

Title

Simple evaluation method for CYP3A4 induction from human hepatocytes; The relative factor approach with an induction detection limit concentration based on the E_{max} model

Shino Kuramoto, Motohiro Kato, Hidetoshi Shindoh, Akihisa Kaneko, Masaki Ishigai and Seiji Miyauchi

Research Division, Chugai Pharmaceutical Co., Ltd., Kanagawa, Japan (S.K., M.K., H.S., A.K., and M.I.)

Department of Pharmacokinetics, Toho University School of Pharmaceutical Sciences, Chiba, Japan (S.M.)

DMD Fast Forward. Published on August 18, 2017 as DOI: 10.1124/dmd.117.076349
This article has not been copyedited and formatted. The final version may differ from this version.

Running Title page

Running Title: The relative factor approach based on the E_{max} model

Corresponding author: Shino Kuramoto

Research Division, Chugai Pharmaceutical Co., Ltd.,

200 Kajiwara, Kamakura, Kanagawa 247-8530, Japan

Tel: +81-467-47-6134. Fax: +81-467-45-3470.

Email: kuramotosn@chugai-pharm.co.jp

The number of text pages: 28

The number of tables: 1

The number of figures: 5

The number of references: 15

The number of words

*Abstract***:** 250 words

*Introduction***:** 645 words

*Discussion***:** 1438 words

DMD Fast Forward. Published on August 18, 2017 as DOI: 10.1124/dmd.117.076349
This article has not been copyedited and formatted. The final version may differ from this version.

Abbreviations

AUC, area under the concentration-time curve; C_{ave}, average concentration during the 24-h culture period; CL_{int} hepatic intrinsic clearance; $C_{ss,u}$, average steady-state unbound plasma concentration; DDI, drug-drug interaction; IDL, induction detection limit; IDLC, induction detection limit concentration; E_{max}, maximum induction effect; f_p, unbound fraction in plasma; $f_{u,medium}$, unbound fraction of a compound in the culture medium; PB, phenobarbital; RF, relative factor; RIF, rifampicin; RIS, relative induction score; $SLOPE_{cpd}$, initial slope of induction response curve of a compound

DMD Fast Forward. Published on August 18, 2017 as DOI: 10.1124/dmd.117.076349
This article has not been copyedited and formatted. The final version may differ from this version.

Abstract

We investigated the robustness and utility of the relative factor (RF) approach based on the E_{max} model, which was reported by Kaneko, using mRNA induction data of 10 typical CYP3A4 inducers in cryopreserved human hepatocytes. The RF value is designated as the ratio of the induction detection limit concentration (*IDLC*) for a standard inducer, such as rifampicin (RIF) or phenobarbital (PB), to that for the compound (RF_{RIF} is $IDLC_{RIF}/IDLC_{cpd}$; RF_{PB} is $IDLC_{PB}/IDLC_{cpd}$). An important feature of the RF approach is that the profiles of the induction response curves on the logarithmic scale remain unchanged irrespective of inducers but are shifted parallel depending on the EC_{50} values. A key step in the RF approach is to convert the induction response curve by finding the *IDLC* of a standard inducer. The relative induction score (RIS) was estimated not only from E_{max} and EC_{50} values, but also from those calculated by the RF approach. These values showed good correlation, having a correlation coefficient of over 0.974, which revealed the RF approach to be a robust analysis irrespective of its simplicity. Furthermore, the relationship between RF_{RIF} or RF_{PB} multiplied by steady state unbound plasma concentration and *in vivo* induction ratio plotted using 10 typical inducers gives adequate thresholds for CYP3A4 drug-drug interaction risk assessment. In the light of these findings, the simple RF approach using the *IDLC* value could be a useful method to adequately assess the risk of CYP3A4 induction in human during drug discovery and development without evaluation of E_{max} and EC_{50}.

DMD Fast Forward. Published on August 18, 2017 as DOI: 10.1124/dmd.117.076349
This article has not been copyedited and formatted. The final version may differ from this version.

Introduction

Because a number of drugs have been withdrawn from the market as a result of serious or fatal drug-drug interaction (DDI) that was found post-marketing, the risk of pharmacokinetic DDI is considered an important issue that should be given priority in drug development. DDI is usually caused as a result of inhibition and induction of the family of metabolic enzymes known as cytochrome P450 (P450). The induction of P450 enzymes elicits a remarkable decrease in drug exposure in clinical practice, which results in reduced therapeutic effect or increased concentrations of active metabolites. Of all P450 enzymes, CYP3A4 is the most abundant in the human liver and small intestine, accounting for 30% and 80%, respectively, and it plays a major role in the metabolism of approximately 30% of clinical drugs (Shimada et al., 1994; Thelen and Dressman, 2009; Ohtsuki et al., 2012; Zanger and Schwab, 2013). Thus, evaluating DDI that arises from CYP3A4 induction in the clinical setting is a also crucial step in drug development.

Recently, major pharmaceutical regulatory agencies—the Food and Drug Administration (FDA), European Medicines Agency (EMA), and Ministry of Health, Labor and Welfare (MHLW)—issued guidance or guidelines on investigating DDIs. These documents state the *in vitro* and *in vivo* DDI studies that should be conducted during drug development to investigate the inhibition and/or induction of CYP3A4. The studies on DDI mediated by CYP3A4 inhibition are well-enough established to give a robust prediction of DDI in the clinical setting. However, although the human

DMD Fast Forward. Published on August 18, 2017 as DOI: 10.1124/dmd.117.076349
This article has not been copyedited and formatted. The final version may differ from this version.

cultured hepatocytes assay system is a recommended study for CYP3A4 induction, a standard method for quantitatively predicting the DDI mediated by CYP3A4 induction from *in vitro* data has not been accepted yet.

Thus far, we have demonstrated that using *in vitro* CYP3A4 induction data from cryopreserved human hepatocytes to quantitatively predict CYP3A4 induction in human is possible and have reported a method of predicting CYP3A4 induction risk in the clinical setting (Kato et al., 2005; Kaneko et al., 2010). This prediction method is called the relative factor (RF) approach and uses the E_{max} model to evaluate induction of CYP3A4 activity in human hepatocytes. It is important to note that in the E_{max} model the profiles of the induction response curves on the logarithmic scale remain unchanged by different inducers, but are shifted parallel depending on the EC_{50} values (Fig.1A). Therefore, a key step in the RF approach is to convert the induction response curve by the induction detection limit concentration (*IDLC*) of standard inducers, such as rifampicin (RIF) or phenobarbital (PB). Because of these features, the potential of new chemical entities to induce CYP3A4 can be assessed using only their *IDLC* values. Other approaches to evaluate CYP3A4 induction from *in vitro* induction data have been postulated that use various parameters, such as the relative induction score (*RIS*), C_{max}/EC_{50}, and AUC/EC_{50} (Persson et al., 2006; Ripp et al., 2006; Chu et al., 2009). These approaches critically require values for the ratio of concentration to CYP3A4 induction response or for induction saturation at higher concentration levels. However, it is difficult to adequately evaluate the induction parameters

DMD Fast Forward. Published on August 18, 2017 as DOI: 10.1124/dmd.117.076349
This article has not been copyedited and formatted. The final version may differ from this version.

of new chemical entities that have cytotoxicity, low solubility, or bell-shaped induction (from complex induction and down-regulation profiles) (Zhang et al., 2014; Vermet et al., 2016). In contrast, the RF approach circumvents the above problems by evaluating the induction potential of new chemical entities from their minimal concentrations, using the *IDLC* value (Kaneko et al., 2009).

In the present study, we verified the robustness and utility of the RF approach using the induction data of 10 typical CYP3A4 inducers in cryopreserved human hepatocytes taken from three donors. By the RF approach, we evaluated the potential of CYP3A4 induction at the mRNA level, as well as in enzymatic activity. The results demonstrate that the simple RF approach using the *IDLC* value is a useful method that adequately assesses the risk of CYP3A4 induction in human.

DMD Fast Forward. Published on August 18, 2017 as DOI: 10.1124/dmd.117.076349
This article has not been copyedited and formatted. The final version may differ from this version.

Materials and Methods

Chemicals

RIF, carbamazepine (CRB), phenytoin (PNT), efavirenz (EFV), pleconaril (PLC), sulfinpyrazone (SLF), nifedipine (NFD), Williams' E medium, bovine serum albumin (BSA), gentamicin, ITS+3 liquid media supplement, and HEPES were purchased from Sigma-Aldrich Co. (St. Louis, MO). Dexamethasone (DXM) was purchased from Junsei Chemical Co. Ltd. (Tokyo, Japan), and omeprazole (OMP), PB, dimethylsulfoxide (DMSO), acetonitrile, formic acid, Hank's Balanced Salt Solution (HBSS), and phosphate buffered saline (PBS) were purchased from Wako Pure Chemical Industries Ltd. (Osaka, Japan). The cryopreserved hepatocytes of Donors 1 and 2 were purchased from Biopredic International (Rennes, France) (Donor 1 was Lot No. NON, from a female, 35-year old Caucasian; Donor 2 was Lot No. IZT, from a female, 44-year old Caucasian) and those of Donor 3 from BioreclamationIVT (New York, NY) (Donor 3 was Lot No. HEP187075, from a male, 64-year old Caucasian). The selection criteria for donors was that the increase of CYP3A4 at RIF 10 μM be over 5-fold that at without inducer. The thawing medium and seeding medium were purchased from Biopredic International. Matrigel was purchased from BD Biosciences (Franklin Lakes, NJ). All other chemicals used were of the highest grade available from Wako Pure Chemical Industries Ltd..

Cell Culture

Cryopreserved human hepatocytes were thawed immediately in the thawing medium and centrifuged

DMD Fast Forward. Published on August 18, 2017 as DOI: 10.1124/dmd.117.076349
This article has not been copyedited and formatted. The final version may differ from this version.

at 200 × *g* for 1 min. The cells were resuspended in the seeding medium and were seeded at 4.0×10^4 cells/well in 96-well plates precoated with collagen type I. After 24-h incubation, the hepatocyte seeding medium was exchanged with a culture medium composed of Williams' E medium supplemented with 84 μg/ml gentamicin, 1% ITS+3 liquid media supplement, 1.25 mg/ml BSA, 2 mM glutamine, 10 mM PBS, and 50 μg/ml Matrigel. The cells were maintained in a humidified incubator at 37°C (5% CO_2) for 48 h before CYP3A4 induction experiments began.

CYP3A4 induction experiment

The range of concentration for the inducers in the CYP3A4 induction experiments were as follows: RIF, 0.01–10 μM; CRB, 3–300 μM; PNT, 1–100 μM; EFV, 0.1–10 μM; PLC, 0.1–100 μM; SLF, 1–100 μM; DXM, 3–300 μM; NFD, 0.1–30 μM; PB, 30–1000 μM; OMP, 0.3–30 μM. All inducers dissolved in DMSO were diluted 1000-fold with incubation medium (final DMSO concentration, 0.1% (v/v)) before being used in the CYP3A4 induction experiment. The cells were incubated in the culture medium containing an inducer or a vehicle control (0.1% (v/v) DMSO). The medium was exchanged with fresh medium containing the inducer or vehicle control every 24 h. After induction for 72 h, the cells were washed twice with ice-cold HBSS. The cells were lysed using a QuantiGene sample processing kit for cultured cells from Affymetrix (Santa Clara, CA) and were stored at −80°C until mRNA levels were determined.

Determination of mRNA level

DMD Fast Forward. Published on August 18, 2017 as DOI: 10.1124/dmd.117.076349
This article has not been copyedited and formatted. The final version may differ from this version.

The mRNA level in the cells was determined according to the instructions provided by Affymetrix. The cell lysates (50 μL) were diluted with 30 μL lysis mixture and were mixed with a 20-μL working plex kit (Panel #12117, CYP3A4, and GAPDH as a housekeeping gene). Detecting the mRNA level was performed on a Bio-Plex 200 from Bio-Rad (Berkeley, CA).

Determination of inducer concentration in the culture medium

Each test compound was analyzed by liquid chromatography coupled with tandem mass spectrometry (LC-MS/MS) as follows. Three-μL aliquots of the culture medium were added to 297-μL internal standard solutions containing 200 nM warfarin and verapamil in acetonitrile. The mixtures were centrifuged for 3 min at 10000 × *g*, and supernatants were injected to LC-MS/MS. The LC-MS/MS equipment consisted of a HPLC system from Shimadzu (Tokyo, Japan), two LC-30AD pumps, a Nexera autosampler, and a CTO-20A column oven coupled with 5500QTRAP MS from AB Sciex (MA, USA). A capcell core ADME column (Shiseido, Tokyo, Japan, 2.7 μm, 50 × 2.1 mm) was used as the analytical column. The mobile phase for the analytical column consisted of two solvents, 0.1% formic acid in water and 0.1% formic acid in acetonitrile. The flow rate was set at 0.6 mL/min.

Determination of the unbound fraction of each inducer in the culture medium

The unbound fraction of each inducer in the culture medium was determined using a Single-Use RED (rapid equilibrium dialysis) Plate (Pierce Biotechnology, Rockford, IL). Three hundred μL of the culture medium and 500 μL of PBS buffer were put into each chamber, respectively. The device

was vigorously shaken and incubated at 37°C. After equilibrium was achieved at 37°C (in a 4-hr dialysis), the concentration of the inducer in both chambers was measured by LC-MS/MS analysis, as described above. The unbound fractions of inducers in the cell culture medium ($f_{u,\ medium}$) are summarized in supplemental data (Supp. Table 3).

Estimation of the average concentration of inducers in the culture medium

Twenty-μL aliquots were taken from the culture medium at designated times (24 and 48 h) after the induction experiment began. The concentration of inducers in the culture medium was measured using LC-MS/MS. The time curve for area under the concentration in medium ($AUC_{24\text{-}48}$) was estimated according to the log-linear trapezoidal rule. The average concentration during the 24 h period (C_{ave}) was estimated by dividing $AUC_{24\text{-}48}$ by 24 h.

Evaluation of RF of the induction from the IDLC values

The RF values were calculated as previously described (Kaneko et al., 2009). The level at which the enzyme is significantly induced, called the induction detection limit (IDL), is at 3-fold standard deviation from the control level. Therefore, the *IDLC* value represents the lowest concentration of the compound that significantly induces the enzyme. The initial slope of the induction response curve of a compound ($SLOPE_{cpd}$) was calculated using the lowest concentration (C_{cpd}) to show an induction response that exceeded the IDL as follows,

$$SLOPE_{cpd} = \frac{I_{cpd} - 1}{C_{cpd}} \quad (1)$$

DMD Fast Forward. Published on August 18, 2017 as DOI: 10.1124/dmd.117.076349
This article has not been copyedited and formatted. The final version may differ from this version.

where I_{cpd} represents the fold induction of a compound at C_{cpd} (Fig. 1B).

The induction curve of a compound is a line for which intercept and slope are 1 and $SLOPE_{cpd}$, respectively. Therefore the *IDLC* value of a compound ($IDLC_{cpd}$) is calculated by the following equation.

$$IDLC_{cpd} = \frac{IDL - 1}{SLOPE_{cpd}} = \frac{3SD}{SLOPE_{cpd}} \quad (2)$$

The RF values for CYP3A4 induction were estimated from the *IDLC* values of standard inducers ($IDLC_i$) as follows.

$$RF_i = \frac{IDLC_i}{IDLC_{cpd}} \quad (3)$$

The RF_i represents the RF values estimated with the standard inducer i.

In the RF approach, assuming that the E_{max} values of CYP3A4 induction remain unchanged irrespective of inducers, and induction response curves are shifted parallel depending on the EC_{50} values (Fig. 1A), RF_i is calculated by the following equation using EC_{50} values,

$$RF_i = \frac{IDLC_i}{IDLC_{cpd}} = \frac{EC_{50i}}{EC_{50cpd}} \quad (4)$$

where EC_{50i} is the EC_{50} of a standard inducer and EC_{50cpd} is the EC_{50} of a compound.

Prediction of induction risk of CYP3A4 in clinical settings using the RF approach

The average steady-state unbound plasma concentration of a compound ($C_{ss,u}$) in clinical settings was calculated for each compound, as previously reported (Kato et al., 2005; Ripp et al., 2006), $C_{ss,u}$ is estimated by the following equation,

DMD Fast Forward. Published on August 18, 2017 as DOI: 10.1124/dmd.117.076349
This article has not been copyedited and formatted. The final version may differ from this version.

$$C_{ss,u} = \frac{f_p \times F \times Dose}{CL_{tot} \times \tau} = \frac{f_p \times AUC_p}{\tau} \quad (5)$$

where f_p is unbound fraction in plasma, AUC_p is the area under the plasma concentration–time curve, τ is dosage interval, CL_{tot} is total clearance, and F is bioavailability. Kinetics parameters in Eq.s 5 and 6 were derived from the database in Goodman & Gilman's The Pharmacological Basis of Therapeutics. CL_{tot} was calculated by the following equation,

$$CL_{tot} = \frac{Dose}{AUC_p} = \frac{0.693 \times V_d}{T_{1/2}} \quad (6)$$

the hepatic clearance (CL_h) was estimated from CL_{tot} and the renal clearance (CL_r) using the following equation,

$$CL_h = CL_{tot} - CL_r \quad (7)$$

and the hepatic intrinsic clearance (CL_{int}) was estimated by Eq. 8 based on the well-stirred model.

$$CL_{int} = \frac{R_b \times Q_h \times CL_h}{f_p \times (Q_h - CL_h)} \quad (8)$$

R_b (blood to plasma concentration ratio) and Q_h (blood flow rate) were assumed to be 1 and 1610 mL/min, respectively (Kato et al., 2005).

In vivo induction ratio of CYP3A4 is estimated as the ratio of CL_{int} with or without treatment of an inducer under *in vivo* conditions (Supp. Table 1). The concentration–response of each inducer is converted by multiplying $C_{ss,u}$ by RF_i values. We designated the threshold of *in vivo* induction response of CYP3A4 as 1.25, which corresponds to a 20% decrement in AUC of substrates, as designated by FDA, EMA, and MHLW. To categorize inducers as having negative or positive possibility of inducing

DMD Fast Forward. Published on August 18, 2017 as DOI: 10.1124/dmd.117.076349
This article has not been copyedited and formatted. The final version may differ from this version.

CYP3A4, we first plotted the induction response curve of CYP3A4 against the converted $C_{ss,u}$ ($C_{ss,u}\times RF_i$) for each inducer and found the first and last data points above and below the 1.25 level, respectively called Point Above 1.25 and Point Below 1.25. Then, a lower threshold was assigned at the data point immediately preceding the Point Above 1.25, and an upper threshold was assigned at the data point immediately following the Point Below 1.25 (Fig. 4). Induction response values that fell below the lower threshold were categorized as negative for risk of CYP3A4 induction while values that fell above the upper threshold were categorized as positive. Thus, the intervening region, which included compounds with induction responses around the 1.25 level, included false-positive and false-negative compounds.

Calculation of RIS using E_{max} model and RF approach

Induction responses of CYP3A4 followed the E_{max} model. There are several methods of assessing the risk of CYP3A4 induction in clinical settings, and *RIS* correlation, is recommended in the EMA guideline for risk assessment, is an approach that evaluates the risk of CYP3A4 induction *in vivo* from *in vitro* induction data. *RIS* is calculated by the following equation.

$$RIS = \frac{E_{max}\times [I]}{EC_{50} + [I]} \quad (9)$$

where [I] is the unbound maximum plasma concentration.

In RF analysis using RIF as a standard inducer, E_{max} of a compound is equal to E_{max} of RIF, and EC_{50} of a compound is calculated from the EC_{50} of RIF divided by RF_{RIF}, and RIS_{RF} was defined as the *RIS*

DMD Fast Forward. Published on August 18, 2017 as DOI: 10.1124/dmd.117.076349
This article has not been copyedited and formatted. The final version may differ from this version.

which was calculated using these parameters by the following equation.

$$RIS_{RF} = \frac{E_{\max RIF} \times [I]}{EC_{50RIF}/RF_{RIF} + [I]} \quad (10)$$

To evaluate the adaptability of the RF approach to the E_{max} model, the values for RIS_{RF} were compared with those for *RIS* that were calculated using E_{max} and EC_{50} (RIS_{Emax})

DMD Fast Forward. Published on August 18, 2017 as DOI: 10.1124/dmd.117.076349
This article has not been copyedited and formatted. The final version may differ from this version.

Results

Time profiles of the concentrations of test inducers and their stability in the cell cultures.

The stability of test inducers was determined by measuring their concentration in the culture medium at 24 and 48 h. RIF, CRB, SLF, DXM, and PB showed good stability with over 80% (the percentage of the initial amount) remaining. On the other hand, the remaining amount of NFD was minimal (1.8% already at 24 h) (Supp. Table 2A). The rest of the test inducers PNT, EFV, PLC, and OMP showed moderate stability, which ranged from 25% to 80%. The $f_{u,medium}$ values of test inducers were also determined to be between 0.145 and 1.02 (Supp. Table 3), and the estimated average unbound concentration of inducers is summarized in supplemental data (Supp. Table 2B).

Evaluation of the CYP3A4 induction assay on the mRNA and enzyme activity scales using cryopreserved human hepatocytes

As shown in Fig. 2, the induction response of CYP3A4 at mRNA level correlated well with enzyme activity ($r \geqq 0.866$); most of the data (over 92%) fell within the 2-fold line of unity, irrespective of hepatocyte lot. The relationship of concentration to CYP3A4 induction at the mRNA level is shown in Fig. 3. CYP3A4 was induced in all three lots of human hepatocytes in line with the increase in test inducer concentration, whereas the maximum response of CYP3A4 induction showed variability among donors, with the response in the lot from Donor 3 being lower than that in other lots. The induction parameters were estimated using the E_{max} model and are summarized in Table 1, which shows that the E_{max} values deviated widely. The values for parameters estimated in the present study

DMD Fast Forward. Published on August 18, 2017 as DOI: 10.1124/dmd.117.076349
This article has not been copyedited and formatted. The final version may differ from this version.

(Table 1) ranged within the values reported by others, indicating that the estimates were comparable with others. To standardize the induction response in the three lots of hepatocytes, the *IDLC* values for all inducers were determined. The thresholds for detection of the induction response were a little different between hepatocyte lots (Donor 1, 1.22; Donor 2, 1.71; Donor 3, 1.81), because the IDL was designated as 3-fold the SD of the experimental data. Utilizing RIF and PB as standard inducers, RF_{RIF} and RF_{PB} values were estimated and are summarized in Table 1.

Prediction of CYP3A4 induction risk in human: the relationship between $C_{ss,u}$×RF and in vivo induction ratio in human

The $C_{ss,u}$ values were estimated from clinical data by Eq. 5 and CL_{int} values were estimated by Eq. 8, using *AUC* in the clinical setting. We then evaluated the *in vivo* conversion concentrations of inducers under steady-state conditions ($C_{ss,u}$×RF_i) using the RF_{RIF} or RF_{PB} value. The ratio of $C_{ss,u}$×RF_i of typical CYP3A4 inducers to induction in CL_{int} under *in vivo* conditions is shown in Fig. 4 and Supp. Table 1. The features of the induction response calculated via $C_{ss,u}$×RF_i values in all lots of human hepatocytes show characteristics of the E_{max} model isotherm. The $C_{ss,u}$×RF_i values for the threshold at which a high potential of CYP3A4 induction is elicited are nearly similar in each lot of human hepatocytes, except for the threshold for RIF in that of Donor 2, for which the $C_{ss,u}$×RF_i value is one-third smaller than others (2 nM) (Fig. 4C). Likewise, the threshold of $C_{ss,u}$×RF_i representing significant CYP3A4 induction occurs around 1 nM. We also evaluated *RIS* values (RIS_{RF} and RIS_{Emax} values) of

DMD Fast Forward. Published on August 18, 2017 as DOI: 10.1124/dmd.117.076349
This article has not been copyedited and formatted. The final version may differ from this version.

test inducers based on the RF_{RIF} value and the E_{max} model, respectively, as explained above by Eq.s 9 and 10. The RIS_{RF} values coincided well with the RIS_{Emax} values in the 3 lots of human hepatocytes, with correlation coefficients in Donors 1, 2, and 3 of 0.974, 0.986, and 0.998, respectively, and more than 82% of the relationships ranged within the 3-fold line of unity (Fig. 5). These good correlations indicated the robustness and validity of estimating *RIS* based on the RF_{RIF} values. However, RIS_{RF} values were estimated on the assumption that the E_{max} value remained constant irrespective of the type of inducer. In the case of a partial agonist, the E_{max} value would be lower than that of a full agonist and would result in an overestimation of the E_{max} value and an underestimation of the EC_{50} value by the RF approach. The estimated RIS_{RF} values showed a tendency to be overestimated, which should make us more cautious about interpreting the estimated RIS_{RF} values.

DMD Fast Forward. Published on August 18, 2017 as DOI: 10.1124/dmd.117.076349
This article has not been copyedited and formatted. The final version may differ from this version.

Discussion

The present study validates the RF approach, which uses the *IDLC* value of the inducer to calculate a factor based on the E_{max} model that can predict the induction potential of a metabolic enzyme. In ten compounds chosen as typical inducers, we determined the potential CYP3A4 induction at the mRNA and enzymatic activity and found a good correlation between them (Fig. 2). In contrast, the concentration-dependent responses for the induction of CYP3A4 mRNA deviated somewhat between different human hepatocyte lots (Fig. 3 and Table 1); namely, the absolute values of E_{max} and EC_{50} differed by up to 7-fold and 35-fold, respectively. This deviation may be caused by variability in the potency of an induction response in individual donors or differences in the process of preparing human hepatocytes. We thus advocate normalizing by the RF values to those of the standard inducers RIF and PB to minimize the variability in the induction response. With Eq.3, the RF values can be estimated from the *IDLC* values, which are the minimal concentrations at which a significant induction of CYP3A4 can be detected. Because they are based on the E_{max} model, the RF values can also be defined as the ratio of the EC_{50} value of a compound to that of the standard inducer (Eq. 4).

In drug development, assessing whether a new chemical entity has the potential to induce P450 enzymes is very important. FDA guidance recommends that each company should either set its own threshold for P450 enzyme induction according to the method used, or should evaluate the R_3 value to calculate the extent of decrease in *AUC* when a metabolic enzyme is induced. The R_3 value is

DMD Fast Forward. Published on August 18, 2017 as DOI: 10.1124/dmd.117.076349
This article has not been copyedited and formatted. The final version may differ from this version.

calculated using the following equation, $R_3=1/(1+d\times E_{max}\times[I]/(EC_{50}+[I])$, where [I] is the maximal total systemic inducer concentration in plasma, and d is the scaling factor assumed as 1 for the basic model. Determining the R3 value requires the entire profile of the concentration-induction curve, which hampers the assessment of induction by compounds with poor solubility and/or toxicity. By contrast in the case of the RF approach with cryopreserved hepatocytes, we could evaluate the threshold of induction using ten inducers in the clinical setting, even without a complete concentration-induction curve. Unfortunately, none of the ten inducers used in this study showed toxicity or poor solubility. To assess whether the method is an improvement over current methods in predicting induction potential requires further investigation that includes various compounds with poor solubility and/or toxicity.

The RF values were used to evaluate the conversion concentration against the standard inducers, and the relationship between the conversion concentration and *in vivo* induction ratio revealed typical concentration-response curves (Fig. 4). When assessing CYP3A4 induction risk using RF values, the upper thresholds of different lots of hepatocytes could be evaluated robustly and relevantly; the unbound concentration at steady state corresponding to RIF ($RF_{RIF}\times C_{ss,u}$) was 7.58, 1.99, and 7.58 nM for Donors 1, 2, and 3, respectively; and the unbound concentration corresponding to PB ($RF_{PB}\times C_{ss,u}$) was 5.98, 10.1, and 8.78 μM for Donors 1, 2, and 3, respectively. These thresholds obtained from human cryopreserved hepatocytes are comparable with those we predicted from HepaRG cells in a

DMD Fast Forward. Published on August 18, 2017 as DOI: 10.1124/dmd.117.076349
This article has not been copyedited and formatted. The final version may differ from this version.

previous report, implying that the RF approach is a very robust and valid approach for predicting the CYP3A4 induction risk of a new chemical entity, and will be useful to reduce the differences across experiments and across laboratories (Kaneko et al., 2009). As shown in Fig. 4, the $RF_i \times C_{ss,u}$ values for 30 mg/kg PB fell on or after the upper threshold, and the $RF_i \times C_{ss,u}$ values for 40 mg/kg NFD fell on or before the lower threshold. These $RF_i \times C_{ss,u}$ values for 30mg/kg PB and 40mg/kg NFD could be used to easily set the negative and positive thresholds for each individual donor. The simplicity and convenience in the estimation of the induction thresholds might be a cost-benefit of using the RF approach for DDI studies during drug development.

Previously, Kanebratt and Anderson developed the AUC/F_2 approach to assess induction risk using HepaRG cells (Kanebratt and Andersson, 2008). The AUC/F_2 values are estimated by dividing *AUC* by F_2, where *AUC* is obtained from the clinical data of the test inducer and F_2 is the concentration at which an inducer elicits CYP3A4 mRNA that is 2-fold of the base line. Although a good correlation between *in vitro* and *in vivo* results was obtained using AUC/F_2, Fahmi and Ripp have pointed out an advantage and a drawback in the AUC/F_2 approach (Fahmi and Ripp, 2010). The advantage is that, because F_2 can be visually evaluated just from the increase phase, its value can be estimated from an incomplete *in vitro* concentration-induction curve The drawback of the F_2 method is that when the potency of the induction response is very low, F_2 values are estimated in the region of saturated response, which is above EC_{50} and outside the definitively linear region of the concentration-response.

DMD Fast Forward. Published on August 18, 2017 as DOI: 10.1124/dmd.117.076349
This article has not been copyedited and formatted. The final version may differ from this version.

On the other hand, it is also possible to overcome the problems of limited dose-response curves from values in the initial slope. The use of the initial slope as an index of induction is clearly valid only if relevant *in vivo* drug concentrations are contained within the definitively linear phase of the response curve, in other words, much lower than EC_{50} (Kato et al., 2005). The RF approach sufficiently meets this condition because the *IDLC* is minimal and definitely lower than EC_{50}; the concentrations occur in the region where the induction response shows linear as governed by the E_{max} model, and the reciprocal of the *IDLC* value corresponds to the initial slope of the induction response curve (Fig. 1B). The RF value acts not only as the conversion factor to a standard inducer that elicits the same induction potential, but also as the ratio of the EC_{50} value of the test inducer to that of the standard inducer. Consequently, although the RF approach, like the AUC/F_2 approach, uses only one parameter (*IDLC*), it can provide a robust and valid prediction of relevant *in vivo* induction potency. Indeed, the RIS_{Emax} values corroborated the RIS_{RF} values well (Fig. 5), implying that the RF approach may be comparable with the E_{max} model approach.

In this analysis, the extent of intracellular exposure ($AUC_{intracell,u}$) was an important determining factor of the induction potency; therefore, we needed to be cautious when estimating the stability and unbound concentration in the culture medium. To confirm the stability in the culture medium, we evaluated the average concentrations of inducers, and compared them with their theoretical concentrations (Supp. Table 2). In the present study, most of the inducers did not show a difference

DMD Fast Forward. Published on August 18, 2017 as DOI: 10.1124/dmd.117.076349
This article has not been copyedited and formatted. The final version may differ from this version.

between the average and theoretical concentrations in the culture medium. However, the amounts of NFD, OMP and PLC recovered in the induction experiments were low (Supp. Table 2A). The low recovery of PLC might be attributed to plastic adsorption and metabolism (Sun et al., 2017) . According to in-house data, NFD and OMP did not show the adsorption to plastic material (data not shown), so low recovery of NFD and OMP might be attributed to the metabolism. We should be cautious about interpreting the induction response for NFD, OMP and PLC. The other important factor that accounted for $AUC_{\text{intracell,u}}$ was the unbound fraction in the culture medium. The unbound fraction of most inducers was more than approx. 0.5 (Supp. Table 3), and the theoretical concentrations of inducers corresponded to their intracellular unbound concentrations. Unfortunately, when we determined the induction of CYP3A4 by troglitazone (TRG) and analyzed TRG by the RF approach, it was only outlier in the master curve (data not shown). TRG is well-known for avidly binding to various proteins, which may reduce the unbound concentration in the culture medium substantially and cause the data points of TRG to deviate far from the curve. To accurately predict induction potential by the RF approach, it is essential to confirm the actual concentration of the test compound and its unbound fraction in the culture medium.

To sum up, we have here demonstrated that evaluating data from cryopreserved human hepatocytes by the RF approach can robustly and relevantly predict the risk of DDI from CYP3A4 induction in a clinical setting. Furthermore, RF values obtained from *IDLC* values are very useful for adequately

DMD Fast Forward. Published on August 18, 2017 as DOI: 10.1124/dmd.117.076349
This article has not been copyedited and formatted. The final version may differ from this version.

predicting the relevant *in vivo* induction potency when cellular toxicity and/or poor solubility of a new chemical entity gives a limited dose-induction-response curve. Using the RF approach with cryopreserved hepatocytes can also provide a robust and relevant threshold for induction in the clinical setting that satisfies FDA and EMA guidelines. The simple RF approach using the *IDLC* value has been demonstrated to be a useful method to adequately assess the risk of CYP3A4 induction in human.

Acknowledgements

We thank Ms. Sally Matsuura for her helpful advice in the preparation and language editing of this paper.

Authorship Contribution

Participated in research design: Kuramoto, Kato, Shindoh, and Kaneko

Conducted experiments: Kuramoto

Performed data analysis: Kuramoto, Kato, and Shindoh

Wrote or contributed to the writing of the manuscript: Kuramoto, Kato, Shindoh, Kaneko, Ishigai, and Miyauchi

Reference

Chu V, Einolf HJ, Evers R, Kumar G, Moore D, Ripp S, Silva J, Sinha V, Sinz M, and Skerjanec A (2009) In vitro and in vivo induction of cytochrome p450: a survey of the current practices and recommendations: a pharmaceutical research and manufacturers of america perspective. *Drug Metab Dispos* **37:**1339-1354.

Fahmi OA and Ripp SL (2010) Evaluation of models for predicting drug-drug interactions due to induction. *Expert Opin Drug Metab Toxicol* **6:**1399-1416.

Kanebratt KP and Andersson TB (2008) HepaRG cells as an in vitro model for evaluation of cytochrome P450 induction in humans. *Drug Metab Dispos* **36:**137-145.

Kaneko A, Kato M, Endo C, Nakano K, Ishigai M, and Takeda K (2010) Prediction of clinical CYP3A4 induction using cryopreserved human hepatocytes. *Xenobiotica* **40:**791-799.

Kaneko A, Kato M, Sekiguchi N, Mitsui T, Takeda K, and Aso Y (2009) In vitro model for the prediction of clinical CYP3A4 induction using HepaRG cells. *Xenobiotica* **39:**803-810.

Kato M, Chiba K, Horikawa M, and Sugiyama Y (2005) The quantitative prediction of in vivo enzyme-induction caused by drug exposure from in vitro information on human hepatocytes. *Drug Metab Pharmacokinet* **20:**236-243.

Ohtsuki S, Schaefer O, Kawakami H, Inoue T, Liehner S, Saito A, Ishiguro N, Kishimoto W, Ludwig-Schwellinger E, Ebner T, and Terasaki T (2012) Simultaneous absolute protein quantification of transporters, cytochromes P450, and UDP-glucuronosyltransferases as a novel approach for the characterization of individual human liver: comparison with mRNA levels and activities. *Drug Metab Dispos* **40:**83-92.

Persson KP, Ekehed S, Otter C, Lutz ES, McPheat J, Masimirembwa CM, and Andersson TB (2006) Evaluation of human liver slices and reporter gene assays as systems for predicting the cytochrome p450 induction potential of drugs in vivo in humans. *Pharm Res* **23:**56-69.

Ripp SL, Mills JB, Fahmi OA, Trevena KA, Liras JL, Maurer TS, and de Morais SM (2006) Use of immortalized human hepatocytes to predict the magnitude of clinical drug-drug interactions caused by CYP3A4 induction. *Drug Metab Dispos* **34:**1742-1748.

Shimada T, Yamazaki H, Mimura M, Inui Y, and Guengerich FP (1994) Interindividual variations in human liver cytochrome P-450 enzymes involved in the oxidation of drugs, carcinogens and toxic chemicals: studies with liver microsomes of 30 Japanese and 30 Caucasians. *J Pharmacol Exp Ther* **270:**414-423.

Sun Y, Chothe PP, Sager JE, Tsao H, Moore A, Laitinen L, and Hariparsad N (2017) Quantitative Prediction of CYP3A4 Induction: Impact of Measured, Free, and

Intracellular Perpetrator Concentrations from Human Hepatocyte Induction Studies on Drug-Drug Interaction Predictions. *Drug Metab Dispos* **45:**692-705.

Thelen K and Dressman JB (2009) Cytochrome P450-mediated metabolism in the human gut wall. *J Pharm Pharmacol* **61:**541-558.

Vermet H, Raoust N, Ngo R, Essermeant L, Klieber S, Fabre G, and Boulenc X (2016) Evaluation of Normalization Methods To Predict CYP3A4 Induction in Six Fully Characterized Cryopreserved Human Hepatocyte Preparations and HepaRG Cells. *Drug Metab Dispos* **44:**50-60.

Zanger UM and Schwab M (2013) Cytochrome P450 enzymes in drug metabolism: regulation of gene expression, enzyme activities, and impact of genetic variation. *Pharmacol Ther* **138:**103-141.

Zhang JG, Ho T, Callendrello AL, Clark RJ, Santone EA, Kinsman S, Xiao D, Fox LG, Einolf HJ, and Stresser DM (2014) Evaluation of calibration curve-based approaches to predict clinical inducers and noninducers of CYP3A4 with plated human hepatocytes. *Drug Metab Dispos* **42:**1379-1391.

DMD Fast Forward. Published on August 18, 2017 as DOI: 10.1124/dmd.117.076349
This article has not been copyedited and formatted. The final version may differ from this version.

Legends for Figures

Figure 1. Conceptual diagram of the RF approach. A) shows curves representing the logarithmic expression of *in vitro* induction response to inducer concentration. Rifampicin (RIF) and phenobarbital (PB) were used as standard inducers. B) shows curves representing the linear expression of *in vitro* induction response to inducer concentration. RF_i: relative factor for standard inducer. IDL: induction detection limit. $IDLC_{cpd}$: induction detection limit concentration, the minimum concentration of compound that showed an induction response. P: the lowest concentration to show an induction response that exceeded the IDL. C_{cpd}: concentration at point P. I_{cpd}: induction response at point P. $SLOPE_{cpd}$: initial slope of the induction response curve for which intercept are 1 and pass through the point P

Figure 2. Correlation between CYP3A4 induction at the mRNA level and enzymatic activity in 3 lots of human hepatocytes. Donor 1 (A), Donor 2 (B), Donor 3 (C). Solid line represents unity and dotted lines represent 2-fold line of unity.

Figure 3. The relationship of inducer concentration to CYP3A4 induction response at mRNA level for 3 lots of human hepatocytes (A, Donor 1; B, Donor 2; C, Donor 3). Closed diamond, RIF; closed triangles, CRB; cross, PNT; asterisk, EFV; closed circle, PLC; horizontal bar, SLF; closed square, DXM; open diamond, NFD; open triangles, PB; open square, OMP.

Figure 4 Relationship between $RF_{RIF} \times C_{ss,u}$ (A, C, E, G) or $RF_{PB} \times C_{ss,u}$ (B, D, F, H) and *in vivo* CYP3A4

DMD Fast Forward. Published on August 18, 2017 as DOI: 10.1124/dmd.117.076349
This article has not been copyedited and formatted. The final version may differ from this version.

induction ratio (ratio of CL_{int}) in human for 3 lots of human hepatocytes (A and B, Donor 1; C and D, Donor 2; E and F, Donor 3; G and H, overall data). Grey lines denote the lower and upper thresholds by which negative and positive compounds are categorized. A lower threshold was assigned at the data point immediately preceding the Point Above 1.25, and an upper threshold was assigned at the data point immediately following the Point Below 1.25. AP: Point Above 1.25, which was the first data points which induction response above 1.25 level. BP: Point Below 1.25, which was the last data point which induction response below 1.25. Closed diamond, RIF; closed triangles, CRB; cross, PNT; asterisk, EFV; closed circle, PLC; horizontal bar, SLF; closed square, DXM; open diamond, NFD; open triangles, PB; open square, OMP.

Figure 5 Correlation of *RIS* calculated using the calculated E_{max} and EC_{50} (RIS_{Emax}) with *RIS* calculated using the RF_{RIF} (RIS_{RF}) for 3 lots of human hepatocytes, Donor 1 (A), Donor 2 (B), and Donor 3 (C). Solid line represents unity and dotted lines represent 3-fold line of unity. Closed diamond, RIF; closed triangles, CRB; cross, PNT; asterisk, EFV; closed circle, PLC; horizontal bar, SLF; closed square, DXM; open diamond, NFD; open triangles, PB; open square, OMP.

DMD Fast Forward. Published on August 18, 2017 as DOI: 10.1124/dmd.117.076349
This article has not been copyedited and formatted. The final version may differ from this version.

Table

Table 1

Induction parameters, RF_{RIF}, and RF_{PB} of 10 inducers for 3 lots of human hepatocytes.

	Donor 1				Donor 2				Donor 3			
	E_{max}	EC_{50}	RF_{RIF}	RF_{PB}	E_{max}	EC_{50}	RF_{RIF}	RF_{PB}	E_{max}	EC_{50}	RF_{RIF}	RF_{PB}
RIF	9.36	0.189	1	790	11.4	0.0961	1	5100	3.71	0.543	1	1160
CRB	10.7	80.7	0.00836	6.60	11.9	47.5	0.00099	5.04	3.75	52.4	0.0089	10.4
PNT	6.18	9.3	0.0246	19.4	12.0	39.4	0.00491	25.0	15.9	291	0.0125	14.5
EFV	36.7	50.0	0.0841	66.4	25.5	15.5	0.126	640	5.88	7.57	0.132	153
PLC	3.91	11.9	0.0175	13.8	7.45	36.7	0.00127	6.47	1.98	2.43	0.0397	46.1
SLF	18.0	68.0	0.0131	10.4	6.14	6.62	0.00404	20.6	5.84	21.5	0.0291	33.7
DXM	13.2	9.21	0.0350	27.6	19.2	19.9	0.00579	29.5	6.54	14.0	0.0950	110
NFD	16.9	150	0.00696	5.49	6.47	12.7	0.0190	96.8	2.26	4.32	0.213	247
PB	9.71	179	0.00127	1	18.1	396	0.00020	1	21.1	5000	0.00086	1
OMP	9.96	31.0	0.00295	2.33	13.3	30.9	0.00197	10.0	6.06	14.1	0.0904	105

E_{max} and EC_{50} were estimated by a simple E_{max} model with WinNonlin 7.0

DMD Fast Forward. Published on August 18, 2017 as DOI: 10.1124/dmd.117.076349
This article has not been copyedited and formatted. The final version may differ from this version.

Figures

Figure 1

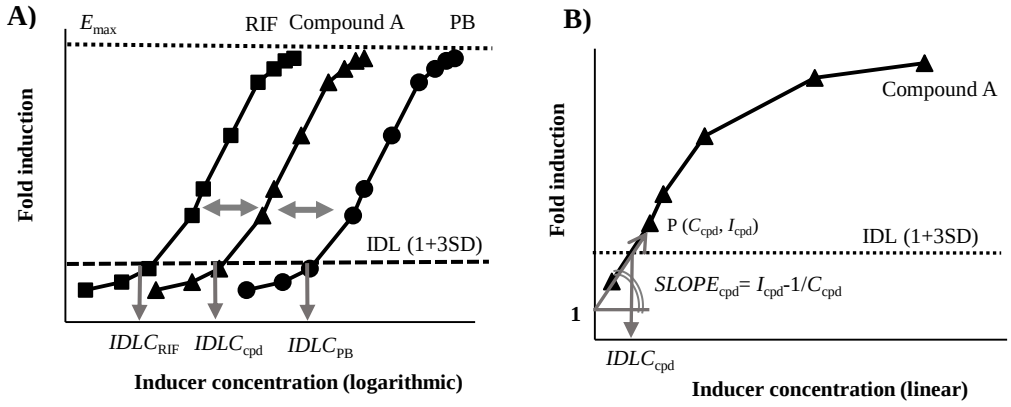

DMD Fast Forward. Published on August 18, 2017 as DOI: 10.1124/dmd.117.076349
This article has not been copyedited and formatted. The final version may differ from this version.

Figure 2

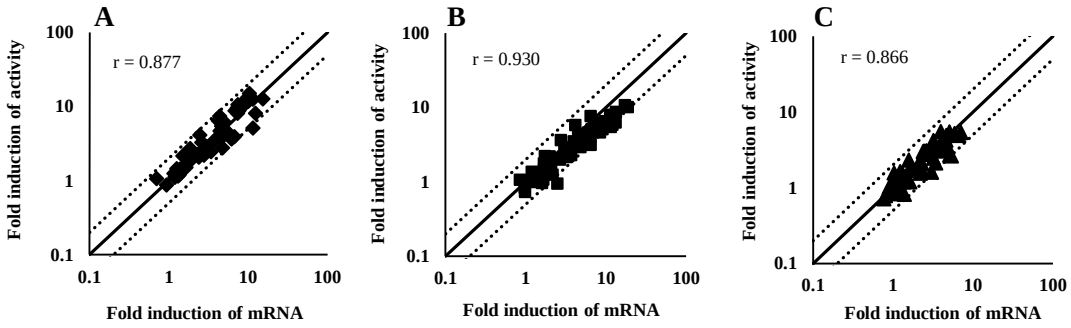

DMD Fast Forward. Published on August 18, 2017 as DOI: 10.1124/dmd.117.076349
This article has not been copyedited and formatted. The final version may differ from this version.

Figure 3

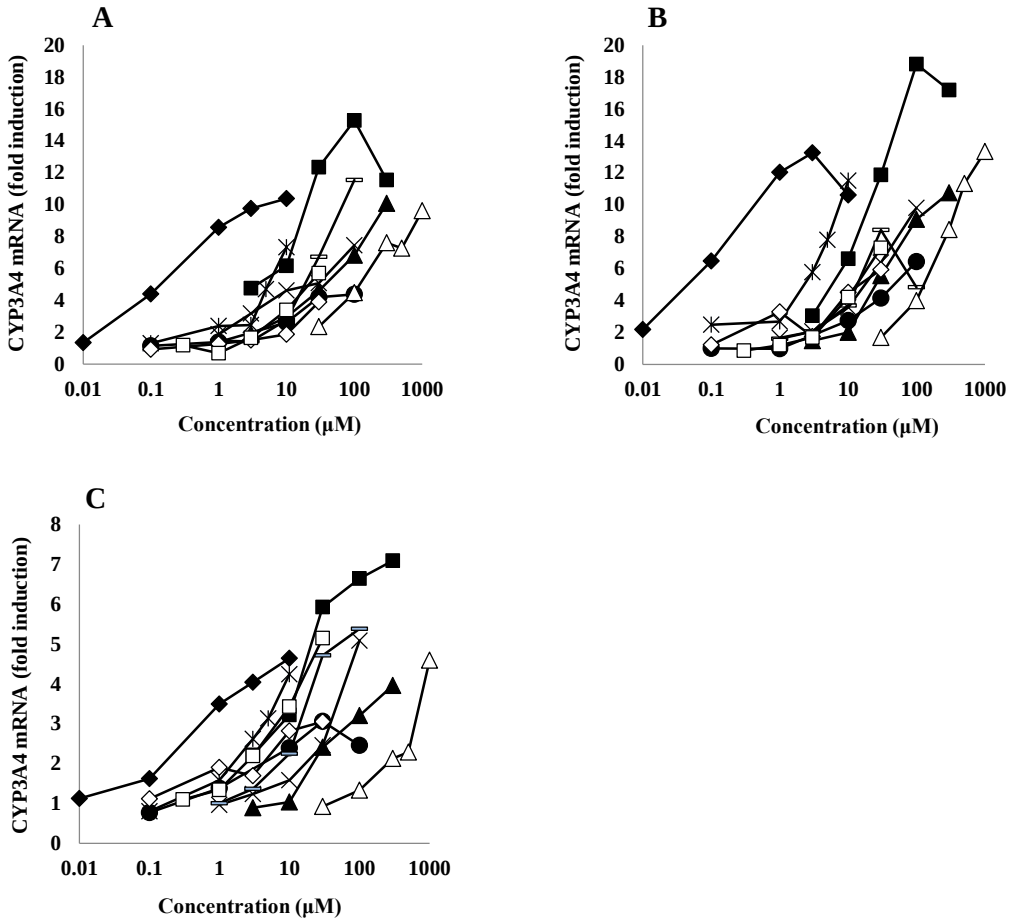

DMD Fast Forward. Published on August 18, 2017 as DOI: 10.1124/dmd.117.076349
This article has not been copyedited and formatted. The final version may differ from this version.

Figure 4

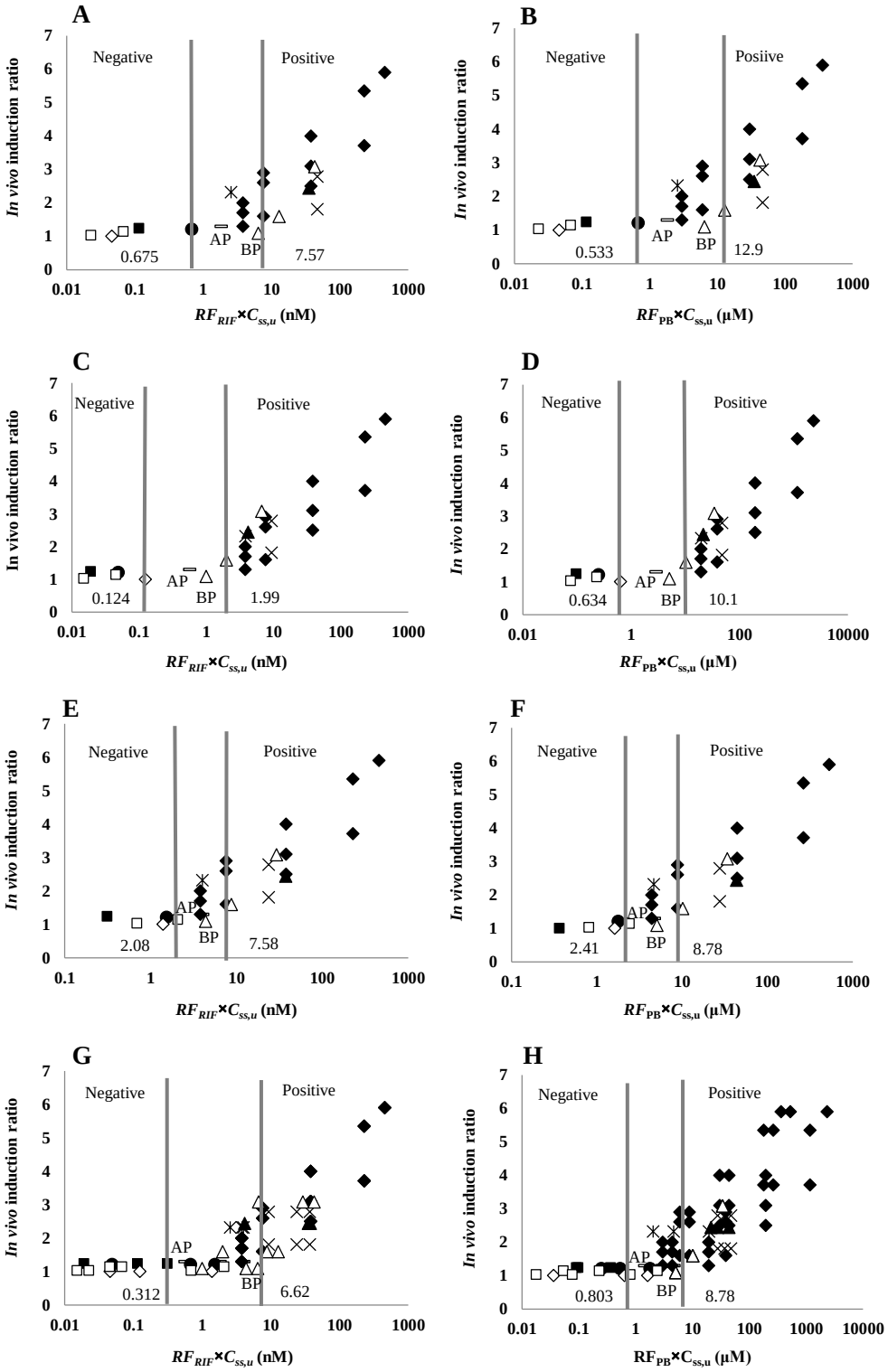

DMD Fast Forward. Published on August 18, 2017 as DOI: 10.1124/dmd.117.076349
This article has not been copyedited and formatted. The final version may differ from this version.

Figure 5